alkylperoxo complexes include (i) the independent synthesis of the *tert*-butylperoxo derivative, $\{\eta^3\text{-HB(3-Bu}^t\text{pz)}_3\}\text{MgOOC(CH}_3)_3$, by the reaction of $\{\eta^3\text{-HB(3-Bu}^t\text{pz)}_3\}\text{MgCH}_3$ with $(CH_3)_3COOH$ (eq 3), and (ii) the formation of the alkoxo derivative $\{\eta^3$-HB-(3-Bu^{t}pz)$_3\}$MgOR[8] and Ph_3PO upon treatment of $\{\eta^3$-HB(3-Bu^{t}pz)$_3\}$MgOOR with PPh_3 (eq 4).

$$\{\eta^3\text{-HB(3-Bu}^t\text{pz)}_3\}\text{MgCH}_3 + (CH_3)_3COOH \rightarrow \{\eta^3\text{-HB(3-Bu}^t\text{pz)}_3\}\text{MgOOC(CH}_3)_3 + CH_4 \quad (3)$$

$$\{\eta^3\text{-HB(3-Bu}^t\text{pz)}_3\}\text{MgOOR} + PPh_3 \rightarrow \{\eta^3\text{-HB(3-Bu}^t\text{pz)}_3\}\text{MgOR} + Ph_3PO \quad (4)$$

Although a number of well-characterized examples of reactions of dioxygen with metal-alkyl complexes have been reported, isolated products are commonly alkoxo derivatives, $[L_nMOR]$,[9] with relatively few examples involving isolation of alkylperoxo complexes, $[L_nMOOR]$.[10] The selective formation of alkylperoxo complexes in the reactions of $\{\eta^3\text{-HB(3-Bu}^t\text{pz)}_3\}$MgR with O_2 is presumably a consequence of the sterically demanding ligand environment that hinders bimolecular oxygen atom abstraction from the alkylperoxo complex by the alkyl derivative, which is the commonly suggested pathway for the formation of alkoxo derivatives (eq 5). In accord with this suggestion, $\{\eta^3$-HB(3-

$$L_nMOOR + L_nMR \rightarrow 2L_nMOR \quad (5)$$

Bu^{t}pz)$_3\}$MgOOCH(CH$_3$)$_2$ and $\{\eta^3\text{-HB(3-Bu}^t\text{pz)}_3\}\text{MgCH(CH}_3)_2$ do not react rapidly at room temperature to give the alkoxo derivative $\{\eta^3\text{-HB(3-Bu}^t\text{pz)}_3\}\text{MgOCH(CH}_3)_2$, but rather require heating to 80 °C to effect this transformation (eq 6).

$$\{\eta^3\text{-HB(3-Bu}^t\text{pz)}_3\}\text{MgOOPr}^i + \{\eta^3\text{-HB(3-Bu}^t\text{pz)}_3\}\text{MgPr}^i \xrightarrow{80\ ^\circ C} 2\{\eta^3\text{-HB(3-Bu}^t\text{pz)}_3\}\text{MgOPr}^i \quad (6)$$

The direct insertion of ground-state triplet oxygen into metal-carbon bonds has been considered to be unlikely since the products would be formed in a high-energy triplet state. Indeed, the rearrangement and racemization of alkyl groups, and inhibition of oxygenation by radical traps, have provided strong evidence for mechanisms involving radical intermediates (eq 7-9) in the reactions of metal-alkyls with O_2.[11] Although the insertion of

$$L_nMR + O_2 \rightarrow L_nMOO^\bullet + R^\bullet \text{ (initiation)} \quad (7)$$

$$R^\bullet + O_2 \rightarrow ROO^\bullet \quad (8)$$

$$L_nMR + ROO^\bullet \rightarrow L_nMOOR + R^\bullet \quad (9)$$

O_2 into the Mg-C bonds of the derivatives $\{\eta^3\text{-HB(3-Bu}^t\text{pz)}_3\}$MgR (R = CH_2CH_3, $CH(CH_3)_2$, $C(CH_3)_3$) is too rapid to be studied, small quantities (<2%) of galvinoxyl, a radical trap, inhibit the reaction $\{\eta^3\text{-HB(3-Bu}^t\text{pz)}_3\}\text{MgCH}_3$ with O_2, thus supporting the above radical-chain sequence for formation of the alkylperoxo derivatives $\{\eta^3\text{-HB(3-Bu}^t\text{pz)}_3\}$MgOOR.

Acknowledgment. Acknowledgment is made to the donors of the Petroleum Research Fund, administered by the American Chemical Society, for partial support of this research.

Registry No. $\{\eta^3\text{-HB(3-Bu}^t\text{pz)}_3\}\text{MgCH}_3$, 122519-72-6; $\{\eta^3\text{-HB(3-Bu}^t\text{pz)}_3\}\text{MgCH}_2\text{CH}_3$, 122519-82-8; $\{\eta^3\text{-HB(3-Bu}^t\text{pz)}_3\}\text{MgCH(CH}_3)_2$, 125950-40-5; $\{\eta^3\text{-HB(3-Bu}^t\text{pz)}_3\}\text{MgC(CH}_3)_3$, 125950-41-6; $\{\eta^3\text{-HB(3-Bu}^t\text{pz)}_3\}\text{MgOOCH}_3$, 125950-42-7; $\{\eta^3\text{-HB(3-Bu}^t\text{pz)}_3\}\text{MgOOCH}_2\text{CH}_3$, 125950-43-8; $\{\eta^3\text{-HB(3-Bu}^t\text{pz)}_3\}\text{MgOOCH(CH}_3)_2$, 125950-44-9; $\{\eta^3\text{-HB(3-Bu}^t\text{pz)}_3\}\text{MgOOC(CH}_3)_3$, 125950-45-0; $\{\eta^3\text{-HB(3-Bu}^t\text{pz)}_3\}\text{MgOCH}_3$, 125950-46-1; $\{\eta^3\text{-HB(3-Bu}^t\text{pz)}_3\}\text{MgOCH}_2\text{CH}_3$, 125950-47-2; $\{\eta^3\text{-HB(3-Bu}^t\text{pz)}_3\}\text{MgOCH(CH}_3)_2$, 125950-48-3; $\{\eta^3\text{-HB(3-Bu}^t\text{pz)}_3\}\text{MgOC(CH}_3)_3$, 122519-77-1.

Supplementary Material Available: Tables of spectroscopic data for all new compounds and tables of crystal and intensity collection data, atomic coordinates, bond distances and angles, and anisotropic displacement parameters and an ORTEP drawing for $\{\eta^3\text{-HB(3-Bu}^t\text{pz)}_3\}\text{MgCH(CH}_3)_2$ (15 pages); listing of observed and calculated structure factors for $\{\eta^3\text{-HB(3-Bu}^t\text{pz)}_3\}\text{MgCH(CH}_3)_2$ (6 pages). Ordering information is given on any current masthead page.

(7) ν_{O-O} for alkylperoxy derivatives are typically in the range 850-950 cm^{-1}. (a) Booth, B. L.; Haszeldine, R. N.; Neuss, G. R. H. *J. Chem. Soc., Dalton Trans.* **1982**, 37-41. (b) Saussine, L.; Brazi, E.; Robine, A.; Mimoun, H.; Fischer, J.; Weiss, R. *J. Am. Chem. Soc.* **1985**, *107*, 3534-3540. (c) Strukul, G.; Ros, R.; Michelin, R. A. *Inorg. Chem.* **1982**, *21*, 495-500. (d) Mimoun, H.; Charpentier, R.; Mitschler, A.; Fischer, J.; Weiss, R. *J. Am. Chem. Soc.* **1980**, *102*, 1047-1054. (e) Strukul, G.; Michelin, R. A.; Orbell, J. D.; Randaccio, L. *Inorg. Chem.* **1983**, *22*, 3706-3713. (f) Momoun, H.; Mignard, M.; Brechot, P.; Saussine, L. *J. Am. Chem. Soc.* **1986**, *108*, 3711-3718. (g) Nishinaga, A.; Tomita, H.; Ohara, H. *Chem. Lett.* **1983**, 1751-1754. (h) Ferguson, G.; Monaghan, P. K.; Parvez, M.; Puddephatt, R. J. *Organometallics* **1985**, *4*, 1669-1674. (i) Giannotti, C.; Fontaine, C.; Chiaroni, A.; Riche, C. *J. Organomet. Chem.* **1976**, *113*, 57-65. (j) Tatsuno, Y.; Otsuka, S. *J. Amer. Chem. Soc.* **1981**, *103*, 5832-5839. (k) van Asselt, A.; Santarsiero, B. D.; Bercaw, J. E. *J. Am. Chem. Soc.* **1986**, *108*, 8291-8293. (l) Mimoun, H.; Chaumette, P.; Mignard, M.; Saussine, L. *Nouv. J. Chim.* **1983**, *7*, 467-475. (m) Espenson, J. H.; Melton, J. D. *Inorg. Chem.* **1983**, *22*, 2779-2781. (n) Giannotti, C.; Fontaine, C.; Septe, B. *J. Organomet. Chem.* **1974**, *71*, 107-124. (o) Nishinaga, A.; Tomita, H.; Nishizawa, K.; Matsuura, T.; Ooi, S.; Hirotsu, K. *J. Chem. Soc., Dalton Trans.* **1981**, 1504-1514.

(8) The alkoxo derivatives $\{\eta^3\text{-HB(3-Bu}^t\text{pyz)}_3\}$MgOR (R = $CH(CH_3)_2$, $C(CH_3)_3$) have also been synthesized independently by the reaction of $\{\eta^3\text{-HB(3-Bu}^t\text{pyz)}_3\}\text{MgCH}_3$ with ROH. Also see ref 3.

(9) (a) Lubben, T. V.; Wolczanski, P. T. *J. Am. Chem. Soc.* **1987**, *109*, 424-435. (b) Brindley, P. B.; Scotton, M. J. *J. Chem. Soc., Dalton Trans.* **1981**, 419-423. (c) Parkin, G.; Schaefer, W. P.; Marsh, R. E.; Bercaw, J. E. *Inorg. Chem.* **1988**, *27*, 3262-3264. (d) Parkin, G.; Bercaw, J. E. *Polyhedron* **1988**, *7*, 2053-2082. (e) Bottomley, F.; Magill, C. P.; White, P. S. *J. Am. Chem. Soc.* **1989**, *111*, 3071-3073. (f) Saussine, L.; Brazi, E.; Robine, A.; Minoun, H.; Fischer, J.; Weiss, R. *J. Am. Chem. Soc.* **1985**, *107*, 3534-3540. (g) Nishinaga, A.; Tomita, H.; Ohara, H. *Chem. Lett.* **1983**, 1751-1754. Also see ref. 2e.

(10) (a) Fontaine, C.; Duong, K. N. V.; Merienne, C.; Gaudemer, A.; Giannotti, C. *J. Organomet. Chem.* **1972**, *38*, 167-178. (b) Chiaroni, A.; Pascard-Billy, C. *Bull. Soc. Chim. Fr.* **1973**, 781-787. (c) Jensen, F. R.; Kiskis, R. C. *J. Organomet. Chem.* **1973**, *49*, C46-C48. (d) Cleaver, W. M.; Barron, A. R. *J. Am. Chem. Soc.* **1989**, *111*, 8966-8967. Also see ref 7n.

(11) (a) Davies, A. G.; Roberts, B. P. *Acc. Chem. Res.* **1972**, *5*, 387-392. (b) Davies, A. G.; Roberts, B. P. *J. Chem. Soc., Dalton Trans.* **1968**, 1074-1078. (c) Lamb, R. C.; Ayers, P. W.; Toney, M. K.; Garst, J. F. *J. Am. Chem. Soc.* **1966**, *88*, 4261-4262. (d) Walling, C.; Cioffari, A. *J. Am. Chem. Soc.* **1970**, *92*, 6609-6611. (e) Howden, M. E. H.; Maercker, A.; Burdon, J.; Roberts, J. D. *J. Am. Chem. Soc.* **1966**, *88*, 1732-1742. (f) Panek, E. J.; Whitesides, G. M. *J. Am. Chem. Soc.* **1972**, *94*, 8768-8775. (g) Jensen, F. R.; Kiskis, *J. Organomet. Chem.* **1973**, *49*, C46-C48. (h) Davies, A. G.; Roberts, B. P. *J. Am. Chem. Soc. B* **1968**, 1074-1078. Als see refs 2e and 9b.

New Nuclear Magnetic Resonance Experiment for Measurements of the Vicinal Coupling Constants $^3J_{HN\alpha}$ in Proteins

Dario Neri, Gottfried Otting, and Kurt Wüthrich*

Institut für Molekularbiologie und Biophysik
Eidgenössische Technische Hochschule—Hönggerberg
CH-8093 Zürich, Switzerland

Received October 12, 1989

The NMR[1] method of protein three-dimensional structure determination[2,3] makes use primarily of distance constraints measured with ^{1}H-^{1}H nuclear Overhauser enhancement (NOE) experiments.[4] High-quality structure determinations further

(1) Abbreviations: NMR, nuclear magnetic resonance; 2D, 3D, two-dimensional, three-dimensional; COSY, 2D correlated spectroscopy; BPTI, bovine pancreatic trypsin inhibitor; 434 repressor(1-69), N-terminal DNA-binding domain of the 434 repressor comprising 69 residues; $^3J_{HN\alpha}$, homonuclear vicinal amide proton-C$^\alpha$ proton coupling constant. In the product operator formalism used, H^N denotes an amide proton, H$^\alpha$ a C$^\alpha$ proton, and N a nitrogen-15 spin.

(2) Wüthrich, K.; Wider, G.; Wagner, G.; Braun, W. *J. Mol. Biol.* **1982**, *155*, 311-319.

(3) Wüthrich, K. *NMR of Proteins and Nucleic Acids*; Wiley: New York, 1986.

(4) (a) Wemmer, D. E.; Reid, B. R. *Annu. Rev. Phys. Chem.* **1985**, *36*, 105-137. (b) Kaptein, R.; Boelens, R.; Scheek, R. M.; Van Gunsteren, W. F. *Biochemistry* **1988**, *27*, 5389-5395. (c) Clore, G. M.; Gronenborn, A. M. *Protein Eng.* **1987**, *1*, 275-288. (d) Würthrich, K. *Science* **1989**, *243*, 45-50. (e) Wüthrich, K. *Acc. Chem. Res.* **1989**, *22*, 36-44.

0002-7863/90/1512-3663$02.50/0 © 1990 American Chemical Society

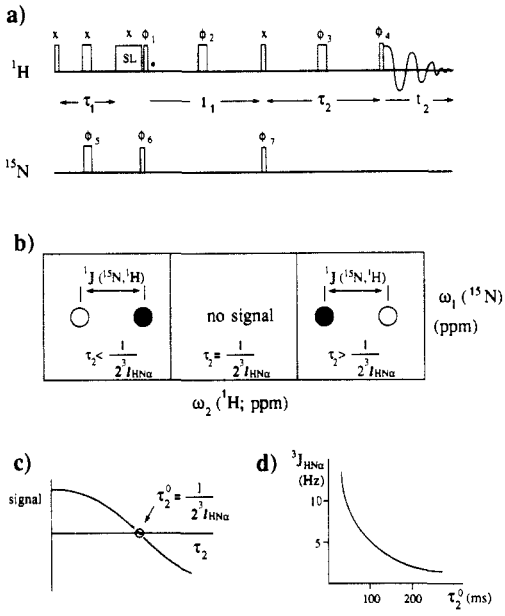

Figure 1. (a) Experimental scheme for measurements of vicinal spin–spin coupling constants $^3J_{HN\alpha}$. It consists of an extension of [^{15}N,^{1}H]-COSY[13a,c] by a delay period τ_2. To ensure observation of all amide protons, the experiment must be performed in H_2O solution.[3] The scheme shown here is therefore preceded by selective irradiation of the water signal.[3] The delay τ_1 is tuned to $1/2\,^1J(^{15}N,^1H)$. Narrow vertical bars indicate $(\pi/2)$ pulses, wide bars are π pulses, and SL denotes a spin-lock purge pulse of 2-ms length.[13c] The following 64-step phase cycle was used: $\phi_1 = (y)_{32}(-y)_{32}$, $\phi_2 = (x,x,-x,-x)_{16}$, $\phi_3 = [(x)_4(-x)_4(y)_4(-y)_4]_4$, $\phi_4 = [(y)_{16}(-y)_{16}]_2$, $\phi_5 = (x)_{64}$, $\phi_6 = (x)_{32}(-x)_{32}$, $\phi_7 = (x,-x)_{32}$, receiver phase = $[(x,-x)_4(-x,x)_4]_4$. The phases ϕ_5 and ϕ_6 were subjected to time proportional phase incrementation (TPPI) for quadrature detection in ω_1.[10a] (b) Schematic presentation of the [^{15}N,^{1}H]-COSY cross-peak fine structure obtained with the experimental scheme of Figure 1a. For each amino acid residue, a cross peak composed of two antiphase components separated along ω_2 by the heteronuclear coupling constant $^1J(^{15}N,^1H)$ is expected; predetermined relative signs of the fine-structure components remain unchanged for mixing periods τ_2 shorter than $1/2^3J_{HN\alpha}$, the signal vanishes for $\tau_2 = 1/2^3J_{HN\alpha} \equiv \tau_2^0$ and the signs are inverted for τ_2 values larger than $1/2^3J_{HN\alpha}$. (c) Time course of the signal intensity for an individual fine-structure component. Only the principal product operator term, $2H_y^NN_z$ (see text) was considered in calculating this curve, and spin relaxation during τ_2 was neglected. (d) Relation between $^3J_{HN\alpha}$ and τ_2^0 computed with the same assumptions as in c.

include measurements of vicinal spin–spin coupling constants as supplementary data.[3,5,6] Of special interest are the amide proton–C$^\alpha$ proton coupling constants $^3J_{HN\alpha}$, since they can be directly related to the polypeptide backbone dihedral angles ϕ.[7,8] In the present paper we propose a novel measurement of $^3J_{HN\alpha}$ in ^{15}N-enriched proteins. The desired information is obtained from the time evolution of the proton coherence at the end of a heteronuclear correlation experiment. This procedure enables measurements of the $^3J_{HN\alpha}$ coupling constants over a wide range of values and promises to significantly improve the precision of the measurement when compared to techniques previously introduced for measurements of proton–proton coupling constants.[9-11] In

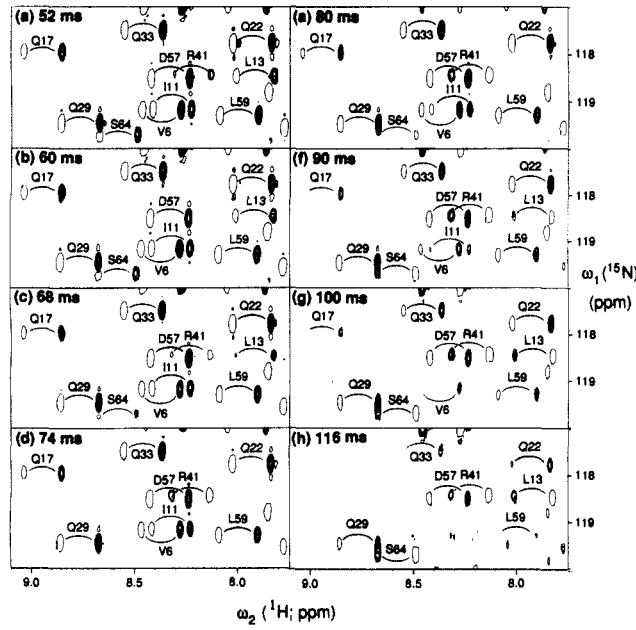

Figure 2. Spectral region (ω_1 = 117–120 ppm, ω_2 = 7.8–9.1 ppm) from eight heteronuclear [^{15}N,^{1}H]-COSY spectra of uniformly ^{15}N labeled 434 repressor(1–69)[15,16] recorded with the experiment of Figure 1a (protein concentration 10 mM in a mixed solvent of 90; H_2O/10% D_2O, 99% ^{15}N enrichment, 25 mM K_2HPO_4 at pH 5.0, 100 mM KCl, T = 28 °C). The individual experiments were recorded with different mixing times τ_2, as indicated in the upper left corner of each spectrum. A Bruker AM-500 spectrometer was used, t_{1max} was 67 ms, and t_{2max} was 160 ms. For each experiment, 160 free induction decays were collected, resulting in a measuring time of 3.5 h. Before Fourier transformation, the time-domain data were multiplied with sine-bell windows[17] along t_1 and t_2, with phase shifts of $\pi/5$ and $\pi/9$, respectively. Positive peak components are plotted with several contour levels and negative components with a single contour level to permit easy identification of the relative signs. Each cross peak is identified by a curved line connecting the two antiphase components of the fine structure, which are separated by the heteronuclear coupling constant $^1J(^{15}N,^1H)$ along the ^{1}H frequency axis ω_2 (Figure 1b). The asymmetry of the doublets comes from increased relaxation of the lower field multiplet component due to chemical-shift anisotropy.[19]

particular, as uniformly ^{15}N labeled biosynthetic proteins become available efficiently and at low cost,[12] the experiment should be widely applicable. Since it has the intrinsic high sensitivity and spectral resolution of heteronuclear correlation spectroscopy, i.e., [^{15}N,^{1}H]-COSY,[13] practical applications should also extend to larger proteins, above the size range accessible for measurements of spin–spin coupling constants with homonuclear techniques.[3,10,11]

In the experimental scheme of Figure 1a, the [^{15}N,^{1}H]-COSY pulse sequence described by Otting and Wüthrich[13c] is extended by a mixing period τ_2. The conventional [^{15}N,^{1}H]-COSY experiment[13] selects for the product operator term $2H_y^NN_z$,[1,14] at the beginning of the period τ_2 (Figure 1a). During τ_2 this term evolves into $-2H_y^NN_z \cos(\pi^3J_{HN\alpha}\tau_2) + 4H_x^NH_z^\alpha N_z \sin(\pi^3J_{HN\alpha}\tau_2)$. The last $(\pi/2)(^1H)$ pulse with phase ϕ_4 (Figure 1a) is along the $\pm y$ axis and converts the second term into $4H_z^NH_x^\alpha N_z$, so that $-2H_y^NN_z$ remains as the only coherence that is observable at the amide proton chemical shift (see also below). Its modulation by $\cos(\pi^3J_{HN\alpha}\tau_2)$ enables the presently proposed measurement of the coupling constants $^3J_{HN\alpha}$. The two-dimensional spectrum resulting from the experimental scheme of Figure 1a contains the typical cross-peak fine structure observed in conventional [^{15}N,^{1}H]-COSY spectra, with two antiphase components separated by $^1J(^{15}N,^1H)$

(5) Kline, A.; Braun, W.; Wüthrich, K. *J. Mol. Biol.* **1988**, *204*, 675–724.
(6) Güntert, P.; Braun, W.; Billeter, M.; Wüthrich, K. *J. Am. Chem. Soc.* **1989**, *111*, 3997–4004.
(7) (a) Karplus, M. *J. Am. Chem. Soc.* **1963**, *85*, 2870–2871. (b) Bystrov, V. F. *Prog. NMR Spectrosc.* **1976**, *10*, 41–81.
(8) Pardi, A.; Billeter, M.; Wüthrich, K. *J. Mol. Biol.* **1984**, *180*, 741–751.
(9) (a) Montelione, G.; Wagner, G. *J. Am. Chem. Soc.* **1989**, *111*, 5474–5475. (b) Kay, L. E.; Brooks, B.; Sparks, S. W.; Torchia, D. A.; Bax, A. *J. Am. Chem. Soc.* **1989**, *111*, 5488–5490. (c) Hosur, R. V.; Majumdar, A.; Patel, D. J. *J. Am. Chem. Soc.* **1989**, *111*, 5482–5483. (d) Widmer, H.; Wüthrich, K. *J. Magn. Reson.* **1987**, *74*, 316–336.
(10) (a) Marion, D.; Wüthrich, K. *Biochem. Biophys. Res. Commun.* **1983**, *113*, 967–974. (b) Neuhaus, D.; Wagner, G.; Vasak, M.; Kägi, J. H. R.; Wüthrich, K. *Eur. J. Biochem.* **1985**, *151*, 257–273.
(11) Griesinger, C.; Sørensen, O. W.; Ernst, R. R. *J. Am. Chem. Soc.* **1985**, *107*, 6394–6396.
(12) McIntosh, L.; Dahlquist, F. W. *Quart. Rev. Biophys.*, in press.
(13) (a) Bodenhausen, G.; Ruben, D. *Chem. Phys. Lett.* **1980**, *69*, 185–188. (b) Ernst, R. R.; Bodenhausen, G.; Wokaun, A. *Principles of NMR Spectroscopy in One and Two Dimensions*; Clarendon: Oxford, 1986. (c) Otting, G.; Wüthrich, K. *J. Magn. Reson.* **1988**, *76*, 569–574.
(14) Sørensen, O. W.; Eich, G. W.; Levitt, M. H.; Bodenhausen, G.; Ernst, R. R. *Prog. NMR Spectrosc.* **1983**, *16*, 163–192.

along the ^1H frequency axis ω_2 (Figure 1b). The intensity of the individual fine structure components varies as cos $(\pi^3 J_{HN\alpha}\tau_2)$ and vanishes for $\tau_2^0 = 1/2^3 J_{HN\alpha}$ (Figure 1b,c). In practice, the experiment of Figure 1a is recorded repeatedly with different mixing periods τ_2. Upper and lower bounds on the range of values for the individual coupling constants $^3J_{HN\alpha}$ are determined by the longest τ_2 value for which the antiphase components of the ^{15}N-^1H cross peak conserve the initial signs, and the shortest τ_2 value for which the signs are inverted (Figure 1b).

With uniformly ^{15}N labeled 434 repressor (1-69), a DNA-binding protein consisting of 69 amino acid residues,[15] nine experiments with delays τ_2 of 52, 60, 68, 74, 80, 90, 100, 116, and 134 ms, respectively, were recorded. The spectral region shown in Figure 2 contains cross peaks between ^{15}N and ^{15}N-bound amide protons. The variation of the cross-peak intensities with τ_2 can readily be followed. For example, the cross peak corresponding to Ser 64 is not inverted up to a mixing time of 68 ms, disappears in the spectrum with τ_2 = 74 ms, and is inverted in the spectra with longer mixing times. Similarly, Leu 13 is inverted between 68 and 90 ms, and Arg 41 between 52 and 68 ms. Val 6 and Gln 17 conserve the sign of their cross-peak components unchanged up to 100 ms and vanish at 116 ms, whereas Asp 57 and Gln 22 conserve the same sign in all the spectra displayed, which corresponds to $^3J_{HN\alpha} < 4.3$ Hz. For comparison: in a 2QF-COSY spectrum recorded under the same conditions, no $^3J_{HN\alpha}$ value smaller than 6.5 Hz could be measured in this protein. The complete set of coupling constants $^3J_{HN\alpha}$ in the 434 repressor(1-69) measured with this method was found to coincide closely with the $^3J_{HN\alpha}$ values expected from the crystal structure of the 434 repressor(1-69)[16] (these data will be further discussed elsewhere).

With a small series of about three to four measurements with suitably selected τ_2 values, the experiment of Figure 1a can be used to determine whether a given $^3J_{HN\alpha}$ coupling constant falls into the range typical for α-helices ($^3J_{HN\alpha} < 6.0$ Hz), β-sheets ($^3J_{HN\alpha} > 8.0$ Hz), or conformationally averaged structure (6.0 Hz $\leq {}^3J_{HN\alpha} \leq 8.0$ Hz).[8] This is usually sufficient for the preparation of the input for a high-quality protein-structure determination.[3-6] For more precise measurements of $^3J_{HN\alpha}$, two additional factors must be considered. First, one would have to account for the fact that other coherences besides $2H_y^N N_z$ are present at the outset of the τ_2 period (Figure 1a). These come from the evolution of the amide proton magnetization under $^3J_{HN\alpha}$ during the short delay τ_1. It can be shown that these additional terms cause a systematic increase of the measured, apparent $^3J_{HN\alpha}$ values by about 6% over the actual values of $^3J_{HN\alpha}$. Second, spin relaxation must be taken into account. With the inclusion of these two factors, the time course between the individual data points recorded at different τ_2 values could be fitted with an analytical function. This interpolation would allow the precise determination of τ_2^0 also between the discrete τ_2 values measured. In addition, the fit could be used to extrapolate experimental measurements at short τ_2 values to longer times, to determine the τ_2^0 values corresponding to small coupling constants $^3J_{HN\alpha}$ (Figure 1d). For small coupling constants, the main limitation of the experiment of Figure 1a results from the long delays τ_2 needed (Figure 1d), since spin relaxation will then greatly reduce its sensitivity.

The experimental scheme of Figure 1a can be extended by insertion of a $\pi(^{15}N)$ pulse at a time $\tau_1/2$ after the end of the evolution period t_1. This additional pulse refocuses the heteronuclear antiphase magnetization, so that ^{15}N broadband decoupling can be applied during the acquisition time t_2. In this version of the experiment, the phase ϕ_4 of the last $(\pi/2)(^1H)$ pulse must be along the x axis rather than along the y axis (see Figure 1a). Compared to the experiment of Figure 1a, the ^{15}N-decoupled spectrum can yield improvements in both sensitivity and resolution.

In a three-dimensional implementation of the experiment in Figure 1a, i.e., 3D J-resolved [^{15}N,^1H]-COSY, the delay τ_2 would be systematically incremented independently of the evolution period t_1 and a Fourier transformation along τ_2 would yield a third frequency dimension. The resulting spectrum consists of several [^{15}N,^1H]-COSY planes, with the peaks spread in the third dimension by $^3J_{HN\alpha}$. The multiplets along the $^3J_{HN\alpha}$ dimension have pure absorptive line shapes. For incompletely resolved multiplets, one would therefore encounter difficulties in a quantitative evaluation of $^3J_{HN\alpha}$ similar to those in a conventional one-dimensional ^1H NMR spectrum, or a homonuclear J-resolved 2D ^1H NMR spectrum.[18] In practice it appears preferable to measure the τ_2 dependence in the time domain by recording multiple heteronuclear 2D NMR spectra (Figure 2) than to extract the information on $^3J_{HN\alpha}$ from a line-shape analysis in the 3D NMR spectrum.[9d]

(15) (a) Anderson, J.; Ptashne, M.; Harrison, S. C. *Proc. Natl. Acad. Sci. U.S.A.* **1984**, *181*, 1307-1311. (b) Neri, D.; Szyperski, T.; Otting, G.; Senn, H.; Wüthrich, K. *Biochemistry* **1989**, *28*, 7510-7516. (c) Wider, G.; Neri, D.; Otting, G.; Wüthrich, K. *J. Magn. Reson.* **1989**, *85*, 426-431.

(16) Mondragon, A.; Subbiah, S.; Almo, S. C.; Drottar, M.; Harrison, S. C. *J. Mol. Biol.* **1989**, *205*, 189-201.

(17) De Marco, A.; Wüthrich, K. *J. Magn. Reson.* **1976**, *24*, 201-204.

(18) Nagayama, K.; Wüthrich, K. *Eur. J. Biochem.* **1981**, *115*, 653-657.

(19) Guéron, M.; Leroy, J. L.; Griffey, R. H. *J. Am. Chem. Soc.* **1983**, *105*, 7262-7266.

Stereochemistry of Nucleophilic Conjugate Addition. Addition of Ethanol-*d* and 2-Methyl-2-propanethiol-*d* to Ethyl Crotonate[1]

Jerry R. Mohrig,* Sabrina S. Fu, Randall W. King, Ronald Warnet,[2] and Gary Gustafson

Department of Chemistry, Carleton College Northfield, Minnesota 55057

Received November 16, 1989

As part of our effort toward a comprehensive understanding of the stereochemistry of addition and elimination reactions involving conjugated carbonyl compounds, we report that the base-catalyzed additions of ethanol-*d* and 2-methyl-2-propanethiol-*d* to ethyl crotonate demonstrate a surprisingly high stereoselectivity. The $(2R^*,3R^*)/(2R^*,3S^*)$ diastereomeric ratio of the addition products is approximately 10:1. Our results indicate that these nucleophilic additions proceed in two steps and that it is the second step, the protonation of the enolate anion, that determines the stereoselectivity of the reaction.

Although 1,4-conjugate nucleophilic additions to unsaturated carbonyl compounds are among the important reactions in organic synthesis[3] and biochemistry,[4] little has been published about their innate stereochemistry with simple, acyclic molecules.[5-8] In the few reports involving acyclic activated alkenes, all done in organic

(1) Presented in part at the 193rd National Meeting of the American Chemical Society, Denver, CO, April 1987; paper ORGN 91.

(2) Simpson College, Indianola, IA 50125.

(3) (a) Oare, D. A.; Heathcock, C. H. In *Topics in Stereochemistry*; Eliel, E. L., Wilen, S. H., Eds.; Interscience: New York, 1989; Vol. 19, pp 227-407. (b) Duval, D.; Gëribaldi, S. In *The Chemistry of Enones, Part 1*; Patai, S., Rappoport, Z., Eds.; Interscience: New York, 1989; pp 355-469.

(4) Talalay, P.; De Long, M. J.; Prochaska, H. J. *Proc. Natl. Acad. Sci. U.S.A.* **1988**, *85*, 8261-8265.

(5) (a) March, J. *Advanced Organic Chemistry*, 3rd ed.; Wiley: New York, 1985; pp 664-666. (b) Patai, S.; Rappoport, Z. In *The Chemistry of Alkenes*; Patai, S., Ed.; Interscience: New York, 1964; pp 491-501.

(6) (a) Bernhard, W.; Fleming, I.; Waterson, D. *J. Chem. Soc., Chem. Commun.* **1984**, 28-29. (b) Fleming, I.; Lewis, J. J. *J. Chem. Soc., Chem. Commun.* **1985**, 149-151. (c) Fleming, I.; Hill, J. H. M.; Parker, D.; Waterson, D. *J. Chem. Soc., Chem. Commun.* **1985**, 318-321. (d) Yamamoto, Y.; Maruyama, K. *J. Chem. Soc., Chem. Commun.* **1984**, 904-905. (e) Kawasaki, H.; Tomioka, K.; Koga, K. *Tetrahedron Lett.* **1985**, *26*, 3031-3034. (f) Takaki, K.; Maeda, T.; Ishikawa, M. *J. Org. Chem.* **1989**, *54*, 58-62.

(7) Heathcock, C. H.; Henderson, M. A.; Oare, D. A.; Sanner, M. A. *J. Org. Chem.* **1985**, *50*, 3019-3022.

(8) Marchese, G.; Naso, F.; Schenetti, L.; Sciacovelli, O. *Chim. Ind. (Milan)* **1971**, *53*, 843-845.

0002-7863/90/1512-3665$02.50/0 © 1990 American Chemical Society